JOURNAL OF CATALYSIS 156, 85–95 (1995)

Study of Pt-Promoted Cobalt CO Hydrogenation Catalysts

D. Schanke,* S. Vada,* E. A. Blekkan,† A. M. Hilmen,† A. Hoff,* and A. Holmen†,[1]

†*Department of Industrial Chemistry, Norwegian Institute of Technology, University of Trondheim, N-7034 Trondheim, Norway; and* **SINTEF Applied Chemistry, N-7034 Trondheim, Norway*

Received March 1, 1994; revised April 5, 1995

The influence of small amounts of Pt on supported Co catalysts has been investigated by several methods. Catalysts containing 9 wt.% Co and 0 or 0.4 wt.% Pt on Al_2O_3 or SiO_2 were prepared by coimpregnation. At $T = 483$ K, $P = 1$ bar, and $H_2/CO = 7$, CO hydrogenation rates (based on weight of cobalt) for Pt-promoted catalysts were 3–5 times higher than those on their unpromoted analogues. The selectivity was not influenced by the presence of Pt. TPR-studies have shown that the presence of Pt strongly influences the reducibility of the catalysts, with TPR-peaks shifting to lower temperatures for all catalysts. This effect is most pronounced on the Al_2O_3-supported catalysts, where the highly dispersed and otherwise difficult to reduce surface cobalt oxides are readily reduced at normal reduction temperatures (623 K) in the presence of Pt. The dispersion of metallic cobalt on Pt promoted catalysts increased compared to that on the unpromoted catalysts, with Al_2O_3-supported catalysts showing the largest effect due to the reduction of highly dispersed surface cobalt oxide. Apparent turnover numbers (based on H_2-chemisorption) were higher for Pt-promoted catalysts than for their unpromoted analogues by a factor of $\simeq 2$. Decoupling coverage and intrinsic reactivity effects on the apparent turnover number by the use of steady-state isotopic transient kinetic analysis revealed essentially constant true turnover numbers on all catalysts. Thus, the increased apparent turnover numbers on Pt-promoted catalysts are due to a higher coverage of reactive intermediates.

1. INTRODUCTION

A key element in improved Fischer–Tropsch processes for natural gas conversion is the development of active cobalt catalysts with high wax selectivity. Many recently developed catalyst systems contain small amounts of a transition metal (typically a noble metal) in addition to cobalt (1). Higher noble metal/cobalt ratios have been reported to give increased oxygenate selectivity (2).

Recent investigations indicate that Fischer–Tropsch synthesis and methanation on cobalt catalysts belong to the class of structure-insensitive reactions, with turnover frequencies essentially independent of the cobalt dispersion and the nature of the support (3, 4). The influence of (noble) metal promoters on the intrinsic catalytic properties of supported cobalt catalysts in the Fischer–Tropsch synthesis has not been extensively studied. However, there has been some work on the characterization and the use of related systems. Batley *et al.* (5) showed that the reduction of metal oxides like Co_3O_4 is influenced by Pt. Similar conclusions were drawn by Belousov *et al.* (6) for Co_3O_4 promoted by Pd. Sass *et al.* (7) studied the Al_2O_3-supported Co–Pd system and found both an increased reducibility of Co and an increased tendency toward Co^{2+} oxidation to Co^{3+} during reoxidation of reduced samples. Guczi and co-workers (2, 8, 9) studied Co–Pt (total metal loading 10 wt.%) catalysts with high Pt:Co ratios. Their findings include a Pt-assisted mechanism for reduction of Al_2O_3-supported Co catalysts and a stabilization of Co ions on the Al_2O_3 surface. The presence of Co–Pt bimetallic particles was inferred from a lower catalytic activity (compared with the monometallic Co catalyst) in the synthesis of hydrocarbons from CO and H_2 (2). Zyade *et al.* (10) also characterized similar catalysts and found (by EXAFS) bimetallic particles with a Pt–Co interatomic distance of 0.271 nm. A similar conclusion was drawn by van't Blik *et al.* in the case of Co–Rh/SiO_2 studied by EXAFS (11), temperature-programmed reduction (TPR), and other techniques (12). Dees and Ponec (13) studied Co–Pt catalysts supported on silica and alumina, with 5 wt.% total metal loading and varying (but high) Pt:Co ratios. X-ray diffraction (XRD) was used to identify alloy formation on silica, although only a part of the cobalt could be accounted for in the alloy. Bardi *et al.* (14, 15) investigated various properties of Co–Pt alloy single-crystal surfaces. While the [111] and [100] surfaces of a $CoPt_3$ alloy have an outermost layer that is essentially pure Pt (14), the [100] surface of a Co–Pt alloy (19 mol% Co) was found to form a layer of CoO when exposed to CO (15).

Many of the kinetic studies of (noble) metal-promoted cobalt have been performed with oxygenate synthesis as the goal. Takeuchi *et al.* (16–18) studied Co–X/SiO_2

[1] To whom correspondence should be addressed.

0021-9517/95 $12.00

catalysts, where X was Ir, Ru, or Re. These metals were found to have similar promoter properties (enhancing the CO hydrogenation rate and oxygenate selectivities) in spite of their very different CO hydrogenation properties when used alone. Ru and Ir added to cobalt catalysts prepared from $Co_2(CO)_8$ gave no significant effect on the activity (19). An enhancement of the activity of cobalt with the addition of small amounts of Ir was found by Guczi *et al.* (20), and Lapidus *et al.* reported a similar effect for Pd addition to supported Co (21).

The present study attempts to explain the role of Pt as a promoter for hydrocarbon synthesis on alumina-supported and silica-supported cobalt catalysts. In addition to conventional measurements of kinetics and metal surface areas, direct information on reaction rates and surface coverage of reaction intermediates has been obtained by the use of steady-state transient kinetic analysis (SSITKA) experiments (22, 23).

2. EXPERIMENTAL

2.1. Catalyst Preparation

Al_2O_3 (Vista Chemicals, 179 m^2/g) and SiO_2 (Davison grade 59, 241 m^2/g) supported catalysts containing ≃9 wt.% Co and 0 or 0.4 wt.% Pt were prepared by incipient wetness coimpregnation of the supports with aqueous solutions of $Co(NO_3)_2 \cdot 6H_2O$ and $Pt(NH_3)_4(NO_3)_2$. The catalysts were dried in air overnight at 393 K and screened to 75–300 μm before calcination in flowing air at 673 K for 2 h. Further pretreatment was done *in situ*. A bulk Co_3O_4 catalyst was also prepared for use as a reference material in TPR studies. NH_3 was added to an aqueous solution of $Co(NO_3)_2 \cdot 6H_2O$ with continuous stirring until there was an excess of NH_3. The precipitate was washed several times in distilled water and dried overnight at 370 K before calcination in flowing air at 643 K for 3 h.

2.2. H_2 Chemisorption

H_2 adsorption isotherms were measured at 298 K in a standard volumetric glass apparatus capable of a vacuum of 10^{-5} Torr or better. Before measurements, the catalysts were reduced in flowing H_2 (1 bar, GHSV ≃ 10000 cm^3(STP)/g catalyst · h) with temperature programming from ambient temperature to 623 K at a rate of 2 K/min and kept at this temperature for 14 h. The samples were then evacuated for ≃0.5 h at 603 K before cooling to 298 K and the adsorption isotherm between 10 and 300 Torr was measured. Strongly and weakly held hydrogen were separated by measuring a second isotherm after pumping for 20 min, but only the results from the first isotherm (total H_2 adsorbed) are reported here. The amount of hydrogen chemisorbed was determined by extrapolating the linear portion of the isotherm to zero pressure.

2.3. Temperature-Programmed Reduction

TPR experiments were performed in a quartz microreactor heated by an electrical furnace. The maximum temperature was 1203 K, and the samples were studied at a heating rate of 10 K/min in a mixture consisting of 7% H_2 in Ar. The H_2 consumption was measured by analyzing the effluent gas with a thermal conductivity detector. Calibration was made both by injecting calibrated pulses of H_2 and by reducing Ag_2O powder. The apparatus has been described in detail elsewhere (24).

2.4. O_2 Titration

The extent of cobalt reduction was determined by O_2 titration of reduced samples at 673 K (25). After reduction under standard conditions (as described above for H_2 chemisorption), the catalysts were kept in flowing Ar at 673 K for 1 h to desorb any chemisorbed H_2. Calibrated pulses of O_2 were then added until no further consumption of O_2 could be detected by a thermal conductivity detector located downstream of the reactor. Extents of reduction were calculated assuming stoichiometric conversion of metallic Co to Co_3O_4.

2.5. X-Ray Diffraction

X-ray diffraction studies were performed in a Philips PW 1710 spectrometer. The studies were aimed mainly at measuring Co_3O_4 particle sizes by XRD line broadening, and all samples were therefore studied either after calcination or after reduction and subsequent reoxidation. Reduced–oxidized catalysts were prepared by passivating used samples from chemisorption experiments in air at 298 K and by oxidizing in air at 468 K for ≃24 h. Co_3O_4 was the only cobalt phase detected by XRD for both calcined and reduced–reoxidized catalysts. Average Co_3O_4 particle sizes were calculated from the most intense Co_3O_4 line ($2\theta = 36.9°$), using the Scherrer formula.

Instrumental line broadening was corrected by calibration with a W standard. In order to compare Co_3O_4 particle sizes with metal dispersions measured by chemisorption, Co_3O_4 particle sizes were converted to the corresponding cobalt metal particle sizes according to the relative molar volumes of metallic cobalt and Co_3O_4. The resulting conversion factor for the diameter d of a given Co_3O_4 particle being reduced to metallic cobalt is

$$d(Co^0) = 0.75 \cdot d(Co_3O_4).$$

Dispersions (D) can be calculated from average metal particle sizes, assuming spherical, uniform particles with site density 14.6 atoms/nm^2, by use of the formula (26)

$$D = 96/d \quad [D = \%, d = \text{nm}].$$

2.6. Steady-State Kinetic Experiments

Kinetic measurements were carried out in the steady-state mode using a quartz fixed-bed reactor operating at atmospheric pressure. Catalyst (50–200 mg) (75–300 μm) was diluted with an inert material (nonporous SiC) in a 1 : 5 weight ratio to minimize temperature gradients. Before kinetic experiments, the catalyst was reduced using the same procedure as described for H_2 chemisorption. After reduction, the catalysts were cooled to 453 K in flowing H_2 and the feed was switched to a mixture containing 56 mol% synthesis gas with $H_2/CO = 7.3$ and 44 mol% Ar. The reaction temperature was then increased to 483 K at a rate of 1 K/min. On-line gas chromatography (GC) samples were taken at regular intervals and analyzed for CO, CO_2, and C_{1+} hydrocarbons on a HP 5880 gas chromatograph equipped with thermal conductivity (TCD) and flame ionization detectors (FID). Ar (used as an internal standard), CO, CH_4, and CO_2 were analyzed on the TCD after separation by a Carbosieve-packed column. C_1–C_4 hydrocarbons were separated by a 0.53-mm i.d. GS-Q capillary column and detected on the FID. Under the conditions used, C_{5+} hydrocarbons, oxygenates, and CO_2 were not detected. GHSV (cm^3(STP) (H_2 + CO + Ar)/(g catalyst · h)) was varied between 4000 and 14,000 h^{-1} to give 10–20% CO conversion.

2.7. Steady-State Isotopic Transient Kinetic Analysis

Steady-state isotopic transient experiments using synthesis gas containing ^{12}CO or ^{13}CO were carried out in conjunction with the steady-state kinetic experiments described above. After reaching steady-state activity (after 3–6 h of reaction), the feed was switched between $Ar/H_2/^{12}CO$ and $Kr/H_2/^{13}CO$ and the transients of Ar, Kr, $^{12}CO/^{13}CO$, and $^{12}CH_4/^{13}CH_4$ were followed by an on-line quadrupole mass spectrometer (Balzers QMG 420). We have used the analysis given by Biloen *et al.* (22, 27) for an irreversible reaction with a single pool of reaction intermediates. It is assumed that the reversible CO adsorption step is rapid compared to the rate of product formation, meaning that "old" $CO_{(ads)}$ primarily transforms backward after an isotopic switch. This allows use of the simplified treatment described above. Deconvolution of the transients to detect surface heterogeneity or multiple pools (28, 29) of intermediates was not attempted.

The following relations and definitions are used (22):

$$\tau_i = \frac{N_i}{R_i} = \frac{N_i/N_s}{R_i/N_s} = \frac{\theta_i}{\mathrm{TOF}},$$

where

τ_i = residence time of reaction intermediates leading to product i [s]

N_i = number of reaction intermediates leading to product i

R_i = rate of i formation [molecules/s]

N_s = number of surface atoms

θ_i = fractional coverage of reaction intermediates leading to i

TOF = apparent turnover frequency = R_i/N_s

$1/\tau_i$ = average intrinsic (true) turnover frequency [s^{-1}].

The residence time, τ, is determined directly as the area between the CH_4 transient and the inert tracer transient (Ar or Kr), after correction for the chromatographic effect on CO (22, 27). The chromatographic effect was used to determine the amount of CO adsorbed under reaction and nonreactive conditions. In the latter case, freshly reduced catalysts were cooled in flowing H_2 to 373 K and then exposed to the same reaction mixture as in the CO hydrogenation experiments described above. By switching between $Ar/H_2/^{12}CO$ and $Kr/H_2/^{13}CO$ and following the transients of Ar, Kr, ^{12}CO, and ^{13}CO, the amount of CO adsorbed at these conditions can be determined. The amount of CO adsorbed (N_{CO}) is given as

N_{CO} = (area between CO transient and inert) · (exit CO flow rate).

3. RESULTS AND DISCUSSION

3.1. Catalyst Characterization

3.1.1. Reducibility and distribution of cobalt oxide phases. Temperature-programmed reduction has been widely used for characterizing supported cobalt catalysts (30–32). The interpretation of the TPR results will therefore to some extent be based on published literature on this subject. In general, all TPR experiments resulted in a total H_2 consumption close to values corresponding to 100% reduction of cobalt oxide. The TPR results can therefore also be interpreted quantitatively as estimates of the distribution of various cobalt oxide phases. TPR profiles of the catalysts are shown in Fig. 1. For (unpromoted) Co/Al_2O_3, the major peaks are found at 650 and 990 K, and a poorly defined broader peak is seen around 1200 K (maximum temperature). The small shoulder at 560 K is caused by decomposition of residual cobalt nitrate on the catalyst. The magnitude of this shoulder peak has been shown to depend strongly on calcination conditions (30, 33, 34). There is also a weak shoulder at about 850 K. The TPR of the (unpromoted) Co/SiO_2 catalyst shows only a pair of peaks at 600 and 670 K, no high-temperature peaks, and no residual nitrate peak, indicating that the nitrate is more easily decomposed on the silica support. This difference could be due to a stabilization of the nitrate on the Al_2O_3 support.

From comparison with previous studies and TPR of bulk Co_3O_4 powder (Fig. 1), the peaks at 600–670 K on (unpromoted) Co/Al_2O_3 and Co/SiO_2 have been identified as relatively large, crystalline Co_3O_4 particles, behaving simi-

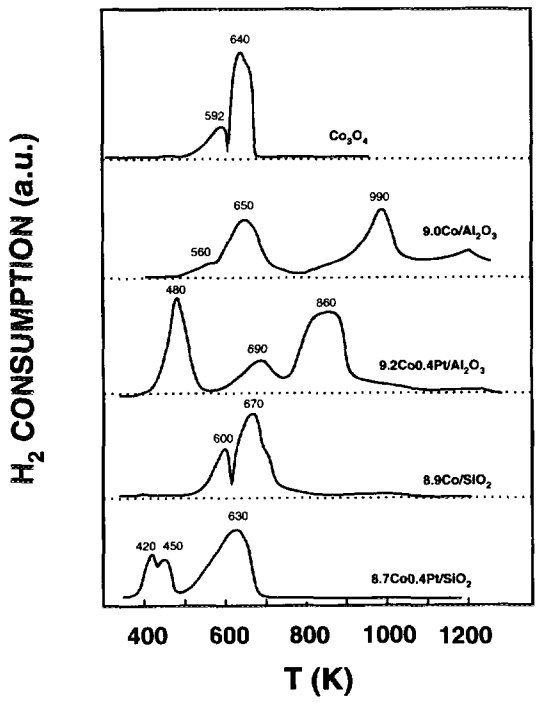

FIG. 1. TPR of supported cobalt catalysts and bulk Co_3O_4. Conditions as described in the text. On reaching 1203 K, the temperature was maintained for approximately 30 min. The portion of the curves above 1203 K signifies the consumption with time at 1203 K.

larly to bulk Co_3O_4. This is also confirmed by the fact that in the calcined (unreduced) catalysts, Co_3O_4 is the only cobalt phase detected by XRD. It has been shown that the two-step reduction of Co_3O_4 (via CoO) to cobalt metal can be seen either as a single peak or two resolved peaks in TPR (30, 32, 34). Unlike Co/Al_2O_3, the Co/SiO_2 catalyst shows two low temperature peaks (at 600 and 670 K), and the 1:3 H_2 consumption ratio for these two peaks (as predicted from the Co_3O_4 reduction stoichiometry) indicates that the two reduction steps are resolved in this case.

The high temperature peak ($\simeq$1200 K) on Co/Al_2O_3 is frequently reported for alumina-supported cobalt catalysts (30, 31) and is usually assigned to a cobalt–aluminum oxide compound, similar to cobalt aluminate ($CoAl_2O_4$). The formation of this compound is a result of solid-state reactions with cobalt ions diffusing into the alumina lattice. The amount of this phase has been reported to be mainly a function of the calcination conditions and is favored by increasing calcination temperatures (30). Under the calcination conditions used in the present study, only a small amount of $CoAl_2O_4$ (or a similar compound) is apparently formed, and $CoAl_2O_4$ is not detected by XRD, as a result of either the low concentration or the lack of long-range ordering.

The peak at 990 K with the shoulder at 850 K observed on Co/Al_2O_3 is very important and seems to be a unique feature of the cobalt–alumina system. In the literature, the cobalt oxide phase giving rise to TPR peaks between 800 and 1000 K has been described as disordered, X-ray amorphous surface overlayers of Co oxide (30, 31). This phase is assumed to be highly dispersed and interacts strongly with the alumina support. The reducibility is intermediate between the larger discrete Co_3O_4 particles (at 650 K) and the $CoAl_2O_4$-like compound (at $\simeq$1200 K). Unlike the latter, the overlayer phase contains a significant fraction of the total amount of cobalt in the Co/Al_2O_3 catalyst (40–50%, estimated from peak areas).

The TPR profiles of the Pt-promoted catalysts are clearly different from the profiles of unpromoted catalysts, in particular for the alumina-supported catalyst. The main pattern with two major peaks is still observed, but the peaks have shifted to lower temperatures by more than 100 K in the case of cobalt on alumina. There is also a third, smaller but clearly resolved peak between the main peaks, possibly corresponding to the low-temperature shoulder on the 990 K peak for Co/Al_2O_3 catalyst. This peak could correspond to an intermediate phase. A range of TPR peaks with different reducibilities due to different degrees of interaction with the surface has been proposed for unpromoted Co/Al_2O_3 (30), and a similar range could be expected with Pt present. On the silica-supported catalyst, which was quite easily reduced also without Pt, the shift in reduction temperatures is smaller for the second peak, presumably representing the reduction of Co^{2+} ions to cobalt metal. The first peak, assumed to arise from the reduction of Co^{3+} to Co^{2+}, is shifted from 600 K to 420–450 K. It should be noted that a separate peak for the reduction of Pt oxide is generally not observed (34). This is due to the high Co/Pt atomic ratio ($\simeq$75) in these catalysts, leading to a very small hydrogen consumption for Pt–oxide reduction compared to the reduction of Co–oxides.

The relative distribution of cobalt oxide in various phases is known to change with preparation and pretreatment conditions (30, 35), but does not seem to be strongly influenced by Pt. The TPR peaks below 700 K (crystalline Co_3O_4 particles) and 800–1000 K (overlayer phase) each represented 40–50% of the total H_2 consumption in the case of Co/Al_2O_3 and $CoPt/Al_2O_3$. The position of the cobalt aluminate peak ($\simeq$1200 K) was not shifted as a result of the presence of Pt. The amount of cobalt aluminate seemed to decrease slightly compared to the Co/Al_2O_3, but was estimated to represent less than 10% of the total amount of cobalt in both cases.

For Co/SiO_2 and $CoPt/SiO_2$, all reduction peaks are located below 700 K, and the cobalt is assumed to be present mainly as Co_3O_4 particles.

These TPR results show clearly that Pt is promoting the reduction of cobalt oxide. Similar results have been reported for $CoPt/Al_2O_3$ (2), $CoRh/Al_2O_3$ (36), $CoIr/Al_2O_3$ (20), $CoRu/CeO_2$ (37), $CoRu/TiO_2$ and $CoRu/SiO_2$

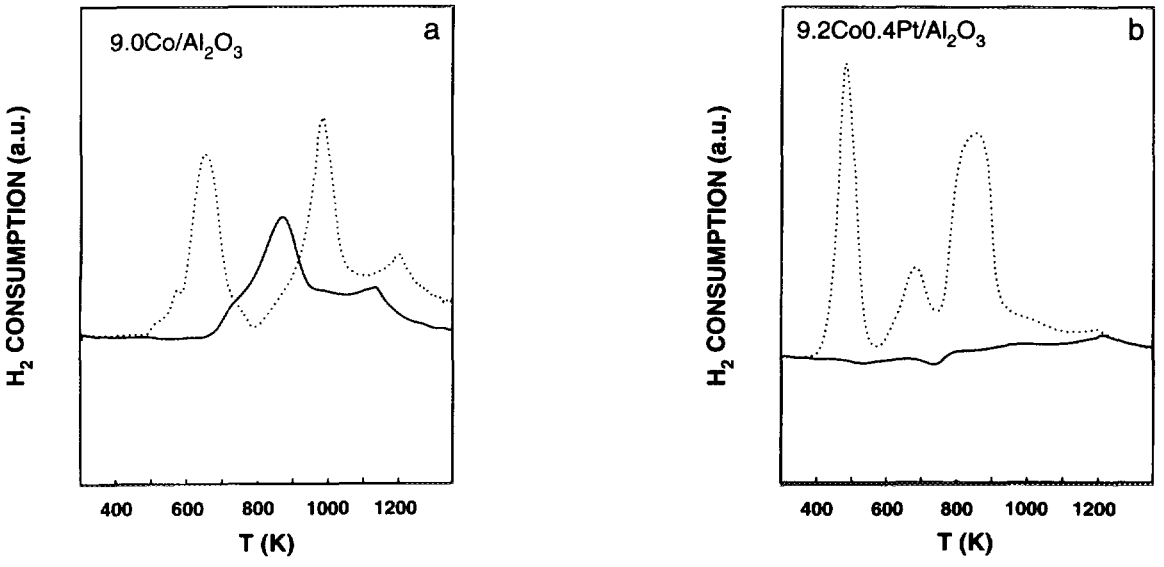

FIG. 2. TPR of prereduced alumina-supported cobalt catalysts (623 K, 16 h) (solid lines). Original TPR of calcined catalysts shown as dotted lines. On reaching 1203 K (1123 K for the reduced Co/Al_2O_3), the temperature was maintained for approximately 30 min. The portion of the curves above 1203 K (1123 K) signifies the consumption with time at 1203 K (1123 K): (a) Co/Al_2O_3 and (b) $CoPt/Al_2O_3$.

(38), and $CoRe/Al_2O_3$ (33, 34). However, the mechanism for this promoting effect is not clear and our study does not give any direct answer to this. A hydrogen spillover effect from Pt to Co is possible, or a more direct interaction between Pt and Co in the form of a Co–Pt interface or bimetallic CoPt particles is possible. If some kind of direct physical contact between cobalt and Pt is necessary for promoting the reduction of cobalt oxides, the small peak at 690 K for $CoPt/Al_2O_3$ can be explained as some remaining cobalt oxide (Co_3O_4) not influenced by Pt.

3.1.2. State of reduction after standard pretreatment. The high-temperature TPR measurements do not give exact information on the extent of reduction after the standard reduction pretreatment used before chemisorption and kinetic experiments. Instead, we have measured this in two different ways; namely, by a modified TPR technique and by reoxidizing reduced samples. The latter method has been widely used for cobalt catalysts (25). The modified TPR consists of a reduction in pure H_2 (1 atm, 623 K, 16 h), followed by a standard TPR to 1203 K. This method has the advantage of showing both the amount and the identity of unreduced cobalt phases, by comparison with the original TPR measurement of unreduced catalysts.

The results are shown in Fig. 2 for cobalt supported on Al_2O_3. In the case of the unpromoted Co/Al_2O_3, the low-temperature peak from the original TPR has disappeared completely in the "new" TPR of the prereduced catalyst. It is recalled that this peak is assumed to represent the discrete, crystalline Co_3O_4 particles. The peaks located at >700 K are still present, although somewhat broader and shifted to lower temperatures. As mentioned before, these have been identified as surface and subsurface cobalt oxides that interact strongly with the alumina support. The hydrogen consumption in the remaining peaks corresponds to roughly 50% of the total hydrogen consumption in the original TPR. This is close to the fraction of cobalt estimated to be present as surface and subsurface cobalt oxides from the standard TPR measurements.

The influence of Pt is clearly demonstrated in Fig. 2b for the $Co–Pt/Al_2O_3$ catalyst. In this case both the low-temperature and the high-temperature peaks are almost completely absent in the "new" TPR of the prereduced catalyst, leaving only a small contribution between 700 and 1200 K. Due to the broadness of this peak and a slightly drifting baseline, the H_2 consumption can only be determined with some difficulty, but is estimated to be $\simeq$10% of the total H_2 consumed in the original TPR.

The TPR observations are supported quantitatively by measuring the extent of reduction by reoxidizing reduced samples in oxygen (Table 1). The extent of reduction is in fair agreement with the values estimated by TPR for the two Al_2O_3-supported catalysts.

Both the unpromoted and the Pt-promoted Co/SiO_2 catalysts show high extents of reduction, as expected from the lack of noticeable H_2 consumption above $\simeq$700 K in TPR (Fig. 1).

From these observations it is concluded that under the reduction conditions used in this study, only the crystalline Co_3O_4 particles are reduced on the unpromoted Co/Al_2O_3 catalyst, corresponding to approximately 50% of the total amount of cobalt present. The distribution of phases is not changed on the $Co–Pt/Al_2O_3$ (relative to the unpromoted

TABLE 1

Characterization Results

Catalyst	Extent of reduction[a] (%)	H_{ads} : Co[b]	H_{ads} : Co[c]	CO : Co[d]	Particle size[e] (nm)	Dispersion (H_2 ads.)[f] (%)	Dispersion (XRD)[g] (%)
9.0Co/Al_2O_3	48	0.033	—	0.013	13.7 (7.6)	6.8	9.4 (16.8)
9.2Co0.4Pt/Al_2O_3	77	0.089 (0.098)[h]	0.077	0.044	14.4 (6.0)	11.5	8.9 (21.4)
8.9Co/SiO_2	90	0.068	—	0.029	19.6 (10.1)	7.5	6.5 (12.6)
8.7Co0.4Pt/SiO_2	92	0.089	0.075	0.052	17.1 (8.6)	9.6	7.5 (15.0)

[a] Determined by reoxidation in O_2 at 673 K (pulse method), assuming $3Co + 2O_2 \rightarrow Co_3O_4$.

[b] Total H_2 chemisorption (mol H/mol Co) at 298 K, assuming adsorption only on Co atoms.

[c] As Footnote *b*, assuming 100% Pt dispersion and adsorption on Co and Pt atoms.

[d] From $^{12}CO/^{13}CO$ transients at 373 K (mol CO/mol Co), assuming adsorption only on Co atoms.

[e] From XRD line broadening. Determined for calcined (unreduced) catalysts. (Results for reduced and subsequently reoxidized catalysts (air, 468 K) given in parentheses.)

[f] Cobalt metal dispersion, given as (H_{ads} : Co)/(fraction reduced), assuming adsorption on Co only.

[g] Calculated from the average particle size of Co_3O_4 as $D(\%) = 96/(0.75d_{Co_3O_4})$ (d = nm) (see Experimental). Determined for calcined (unreduced) catalysts. (Results for reduced and subsequently reoxidized catalysts (air, 468 K) given in parentheses.)

[h] Measured after reduction at 623 K, reoxidation in air at 468 K and reduction at 623 K.

catalyst), but in this case the more highly dispersed overlayers of cobalt oxide are also almost completely reduced under the conditions used. The cobalt–aluminate-like compound (represented by the peak at ≈1200 K) does not seem to be significantly influenced by Pt.

The reason for the shift in the position of the peak representing the remaining oxide in the TPR of the prereduced Co/Al_2O_3 (from 990 K in the original TPR to 890 K for the prereduced catalyst) is not clear. One possibility is that the amount of Co^{2+} in the overlayer phase has increased relative to Co^{3+} as a result of the prereduction treatment. The relative population of Co^{2+}/Co^{3+} has been reported to be sensitive to pretreatment conditions (30), but it is not obvious that this should lead to a lower reduction temperature. A more likely mechanism may be a promotion of the reduction of the overlayer phase by metallic cobalt particles already present initially from the reduction of Co_3O_4 particles. This may be analogous in principle to the observed promotion by Pt of the reduction of cobalt oxides.

3.1.3. Dispersion and particle size. As shown in Table 1, the apparent dispersion measured by H_2 or CO chemisorption is also strongly influenced by the presence of Pt, but the magnitude of the effect depends on the support. For cobalt supported on alumina, the hydrogen uptake is almost tripled as a result of the addition of Pt, whereas a much less pronounced effect of Pt is seen for cobalt on silica. An almost identical trend is shown for CO chemisorption, but the amount of CO adsorbed is always less than for hydrogen by a factor of approximately 2.

XRD line broadening analysis showed significantly larger particle sizes for calcined (unreduced) catalysts than for catalysts that had undergone reduction and reoxidation (see Experimental). The calcined (unreduced) catalysts all showed Co_3O_4 average particle sizes in the range 14–20 nm and with no consistent decreasing trend in particle size for Pt-promoted catalysts. In general, the reduced and reoxidized catalysts had roughly half of the average particle sizes of the calcined catalysts. The results indicated slightly smaller particles for the Al_2O_3-supported catalysts than for their SiO_2-supported analogues. Reduced–reoxidized Pt–promoted catalysts showed ≈20% smaller particles than the unpromoted catalysts for both supports.

In the interpretation of the XRD and chemisorption results, the state of reduction of the catalysts and the ability of XRD to detect various cobalt phases must be considered, as well as the possibility of adsorption on Pt itself. One obvious difficulty is to account for an unknown quantity of H_2 (or CO) adsorbed on "free" Pt. A reliable way of determining adsorption on Co and Pt separately is not easily available. At present, we have chosen to report adsorbed amounts as if all H_2 or CO were adsorbed on Co. The other extreme situation would be the case of Pt existing exclusively as free Pt particles with 100% Pt dispersion. Even in this case, the H_{ads} : Co ratio would only decrease from 0.089 to 0.077 and 0.075 for Co–Pt/Al_2O_3 and Co–Pt/SiO_2, respectively (Table 1). In the present case of coimpregnation with Co and under pretreatment conditions not optimized for maximum Pt dispersion, 100% Pt dispersion seems extremely unlikely. Consequently, the conclusion remains that the increase in the amount of H_2 or CO adsorbed is caused mainly by increased adsorption on cobalt.

The H_{ads} : CO_{ads} ratio $\gg 1$ observed in the present study

may to some extent be caused by a less than monolayer coverage of CO at the low partial pressure of CO (≈50 Torr) used in the SSITKA experiments under nonreactive conditions (see Experimental). In general, H_{ads}:CO_{ads} ratios >1 as well as <1 have been reported on cobalt catalysts, and this ratio has been shown to be sensitive to the dispersion, the extent of reduction, and metal–support interactions (39). The calculations of the fraction of exposed metallic cobalt surface are based on the H_2 adsorption data, a widely accepted method with good agreement with physical methods (XRD,TEM) (3, 26).

In order to calculate the dispersion of the metal phase from chemisorption, it is necessary to multiply the metal loading by the extent of reduction, as outlined by Bartholomew and co-workers (40, 41). This procedure is based on the assumption that unreduced cobalt is present in a separate dispersed phase. The resulting increase in metal dispersion for Co/Al_2O_3 as a result of Pt addition is still significant (Table 1). In the case of Co/SiO_2 and $Co–Pt/SiO_2$, both catalysts are almost completely reduced and the correction for the extent of reduction does not make any difference.

The large deviation between dispersions measured by H_2 chemisorption on reduced catalysts and XRD on reduced–oxidized catalysts is probably caused by a redispersion effect resulting from large cobalt particles breaking up into smaller ones during oxidation, as reported for Co/SiO_2 catalysts by Castner *et al.* (42). This increase in dispersion is probably to some extent lost after a second reduction of a reduced–oxidized catalyst. This is clearly shown by the moderate (≈10%) increase in H_{ads}:Co on a reduced–oxidized–reduced $Co–Pt/Al_2O_3$ catalyst, compared to the more than twofold decrease in particle size (XRD) from the calcined to the reduced–oxidized catalyst (Table 1). Particle sizes measured on reduced-oxidized catalysts are therefore not considered to be representative of reduced catalysts, although qualitatively the same trend is followed for dispersions calculated from chemisorption and XRD. The results reported by Lee *et al.* on Co/Al_2O_3 catalysts (43) also indicate that the dispersion is largely fixed after the calcination step.

There is reasonable agreement between the dispersions calculated from XRD on calcined samples and from H_2 chemisorption for both of the SiO_2-supported catalysts. This confirms the conclusion from TPR that these catalysts mainly contain crystalline Co_3O_4 particles. The dispersion does not seem to change as a result of the reduction.

On the unpromoted Co/Al_2O_3 catalyst, the dispersion calculated from XRD is slightly higher than that measured by H_2 chemisorption. This may indicate that XRD, in addition to the main contribution from large and relatively easily reducible Co_3O_4 particles, detects a small fraction of the highly dispersed, unreduced surface oxides. The reverse situation is observed for $CoPt/Al_2O_3$, with H_2 chemisorption showing a 70% increase in dispersion compared to the unpromoted catalyst, while XRD of the calcined samples showed approximately constant dispersion for Co/Al_2O_3 and $Co–Pt/Al_2O_3$. This again confirms the conclusions from TPR that the presence of Pt facilitates the reduction of the highly dispersed and (largely) X-ray amorphous surface cobalt oxides. The increased dispersion measured by H_2 chemisorption on the $Co–Pt/Al_2O_3$ catalyst is therefore a result of averaging the dispersion of two different cobalt phases. In contrast, XRD detects mainly the large, crystalline Co_3O_4 particles present on both Al_2O_3-supported catalysts. Since the increase in H_{ads}:Co as a result of Pt addition on the Al_2O_3-supported catalyst is far larger than the increase in extent of reduction, this confirms that the dispersion of the overlayer phase is higher than that for the crystalline Co_3O_4 particles.

On the SiO_2-supported catalysts, the effect of Pt on cobalt metal dispersion is small and of the same magnitude as measured by XRD on calcined samples. The possibility of Pt acting as a dispersion improver without influencing the final state of reduction on SiO_2-supported catalysts should therefore not be overlooked. Alternatively, the effect of Pt on the dispersion measured by H_2 or CO chemisorption on reduced catalysts may be a result of the downshift in Co_3O_4 reduction temperatures shown by TPR. This may lead to a more "gentle" reduction process with a smaller tendency to particle agglomeration.

TABLE 2

Steady-State Kinetic Data

Catalyst	r_{CO}[a] (μmol/(g_{Co} · s))	TOF_{CO}[b] (s^{-1})	Hydrocarbon Selectivity[c] (%)		
			CH_4	C_2–C_4	C_{5+}
$9.0Co/Al_2O_3$	4.1	0.0074	66	34	—
$9.2Co0.4Pt/Al_2O_3$	22.7	0.0151	67	33	—
$8.9Co/SiO_2$	7.2	0.0063	62	38	—
$8.7Co0.4Pt/SiO_2$	21.0	0.0140	68	32	—

Note. T = 483 K, P = 1 bar, H_2/CO = 7.3, 44% inert (Ar), 10–20% CO conversion (after 3–6 h of reaction).

[a] CO conversion rate.

[b] CO molecules converted/($H_{ads,298K}$ · s).

[c] Carbon selectivity (CO_2 was not detected).

3.2. Kinetics

The catalytic effect of Pt addition is shown in Table 2. Based on the weight of cobalt, the Pt-promoted catalysts are 3–5 times more active than their unpromoted analogues and the effect is most pronounced for the alumina-supported catalyst. Among the unpromoted catalysts, the Co/SiO_2 catalyst is almost twice as active as the Co/Al_2O_3. For the promoted catalysts the situation is reversed, with

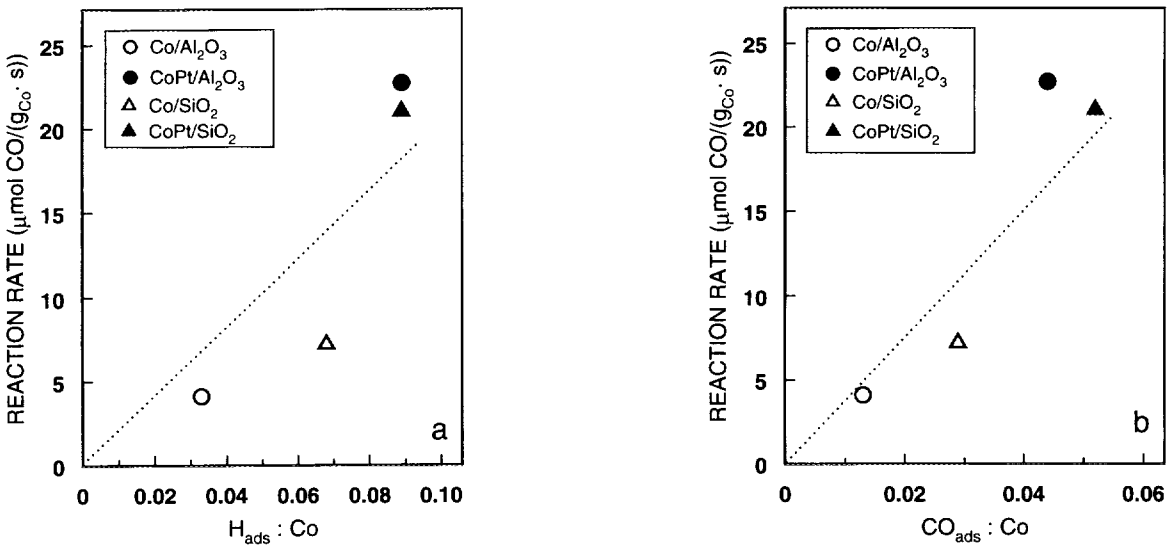

FIG. 3. Steady-state CO hydrogenation rate (based on weight Co) as a function of (a) $H_{ads,298K}$ or (b) $CO_{ads,373K}$. T = 483 K, P = 1 bar, H_2/CO = 7.3, 44% inert (Ar) in feed. CO conversion 10–20% (after 3-6 h of reaction).

$Co–Pt/Al_2O_3$ showing slightly higher activity than $Co–Pt/SiO_2$. The operating conditions (low pressure, high H_2/CO ratio) favor light hydrocarbon formation even at the low temperature used (483 K), and the differences in selectivity between all four catalysts are very small, with 60–70% methane selectivity in all cases.

A plot of the reaction rate (based on the weight of metal) as a function of the amount of hydrogen or CO adsorbed shows that although the reaction rate in general increases with the amount chemisorbed, there is not a perfect straight line relationship (Fig. 3). A straight line through the origin is expected if the turnover number is constant for all the catalysts, provided that H_{ads} : Co or CO_{ads} : Co determines the number of active sites correctly. (The turnover number would then be proportional to the slope of the line.) The apparent turnover numbers, as calculated from steady state rate data and H_2 chemisorption, are nearly independent of the support but increase by a factor of $\simeq$2 for Pt-containing catalysts compared to the unpromoted catalysts (Table 2).

In many reactions involving hydrocarbons or CO, it has been shown that the catalyst surface is largely covered by unreactive material and the reaction is actually occurring on only a small fraction of the total surface. In such cases apparent turnover numbers (based on total exposed surface) do not reflect the true rate of the catalytic event. In addition, low pressure conditions, and in particular high H_2/CO ratios, may lead to significant variations in the surface coverage of reactants and intermediates for different catalysts. At higher pressures and conversions it has been shown that apparent turnover numbers on cobalt catalysts are independent of the support (3), but are increased by addition of a small amount of Ru (38). In the latter case, the effect was attributed to inhibited deactivation as a result of the "cleaning effect" of Ru, leading to a larger active cobalt surface area under reaction conditions.

In order to decouple the effects of intrinsic turnover frequency and surface coverage on the overall (or apparent) turnover frequency, we studied the methanation kinetics by SSITKA. Examples of transients are given in Fig. 4, and the results are summarized in Table 3 and Fig. 5. It is evident from Fig. 5 that the increase in apparent turnover number for Pt-promoted catalysts is accompanied by a similar increase in the coverage of reactive surface intermediates leading to CH_4 (denoted θ_{CH_x}). This is a result of the essentially constant residence times ($\tau \simeq 10$ s) for all the catalysts, measured directly by SSITKA. It can be concluded from this that the increased apparent turnover numbers for the Pt-promoted catalysts are caused by coverage effects and not by increased intrinsic reactivity. The true turnover frequency, as given by $1/\tau$, is close to 0.1 s^{-1} in all four cases, which is similar to 0.10–0.12 s^{-1} measured for bulk Co powder by SSITKA at 488 K, 3 bar total pressure, and H_2/CO = 5 (22). This, together with the insignificant differences in selectivity, indicates that the basic CO hydrogenation catalysis is not influenced by the support or the presence of Pt in the systems investigated here.

The coverage of reaction intermediates leading to CH_4 (θ_{CH_x}) is low in all cases, corresponding to 5–10% of the available surface (measured by H_2 chemisorption). The chromatographic effect indicates a 25–40% coverage of adsorbed CO, and with no particular trend for the promoted/unpromoted catalysts. The total coverage of surface species detected, $\theta_{CO} + \theta_{CH_x}$, is <1.0 in all cases. It is difficult to say whether this indicates a large number of unoccupied sites

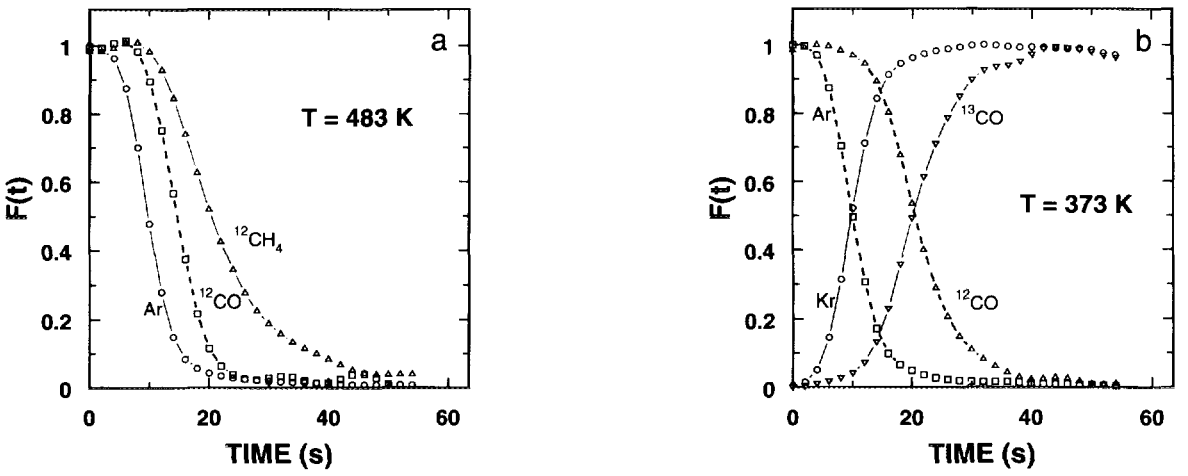

FIG. 4. Example of isotopic transients after switching from Ar/^{12}CO/H_2 to Kr/^{13}CO/H_2 over 9.2Co0.4Pt/Al_2O_3. $F(t)$ = normalized transient response. H_2/CO = 7.3, P = 1 bar, 44% Ar or Kr. (a) During CO hydrogenation at T = 483 K. Only Ar, ^{12}CO and $^{12}CH_4$ responses are shown. (b) Under nonreactive conditions, T = 373 K.

or if the surface is blocked by some other unreactive compound. On the other hand, if the surface coverages are calculated from CO chemisorption under nonreactive conditions (instead of H_2 chemisorption), the surface coverages under reactive conditions account for 70–100% of the CO-adsorbing surface. It is possible that CO chemisorption at 373 K is a more realistic measure of the number of surface sites involved in the Fischer–Tropsch or methanation reaction. It has been shown that certain CO adsorption sites are the sites active for the main CO hydrogenation pathway on cobalt catalysts (44).

Although this study has concentrated on the kinetics for methane formation, it is believed that the same conclusions are generally true also for Fischer–Tropsch synthesis. At the low reaction temperature used (483 K), the selectivity can be varied from almost only methane to high C_{5+} selectivity in a controlled way by adjusting the H_2/CO ratio, even at atmospheric pressure. There is increasing agreement that methane and higher hydrocarbons are formed from a common reaction intermediate, and promoters like Pt would be expected to act similarly in both cases. However, since we have shown that part of the promoter effect is linked to differences in coverage under working conditions, it is also possible that the magnitude of the effects can change with increasing total pressure and decreasing H_2/CO ratio.

4. CONCLUSIONS

The addition of Pt significantly increases the CO hydrogenation rate (based on weight of Co) of Co catalysts supported on Al_2O_3 or SiO_2. The increased rates are caused by: (i) increased reducibility; (ii) increased dispersion of reduced Co particles; (iii) increased coverage of reaction intermediates.

The increased extent of reduction as a result of Pt pro-

TABLE 3

Kinetic Parameters Calculated from SSITKA

Catalyst	$r_{CH_4} \cdot 10^5$ (mol/($mol_{Co} \cdot s$))	TOF_{CH_4}[1] (s^{-1})	$1/\tau_{CH_x}$ (s^{-1})	θ_{CO}[2] (H:Co)	θ_{CH_x}[2] (H:Co)	θ_{CO}[3] (CO:Co)	θ_{CH_x}[3] (CO:Co)
9.0Co/Al_2O_3	16	0.005	0.10	0.25	0.05	0.63	0.12
9.2Co0.4Pt/Al_2O_3	90	0.010	0.10	0.31	0.10	0.63	0.20
8.9Co/SiO_2	27	0.004	0.08	0.38	0.05	0.89	0.12
8.7Co0.4Pt/SiO_2	83	0.009	0.10	0.32	0.09	0.55	0.16

Note. T = 483 K, P = 1 bar, H_2/CO = 7.3, 44% inert (Ar), 10–20% CO Conversion (after 3–6 h of Reaction).

[1] CH_4 molecules formed ($H_{ads,298K} \cdot s$).

[2] Surface coverage: $\theta_i = N_i/H_{ads,298K} \cdot N_i$ (i = CH_x, CO) determined by SSITKA under reaction conditions.

[3] Surface coverage: $\theta_i = N_i/CO_{ads,373K} \cdot N_i$ (i = CH_x, CO) determined by SSITKA under reaction conditions.

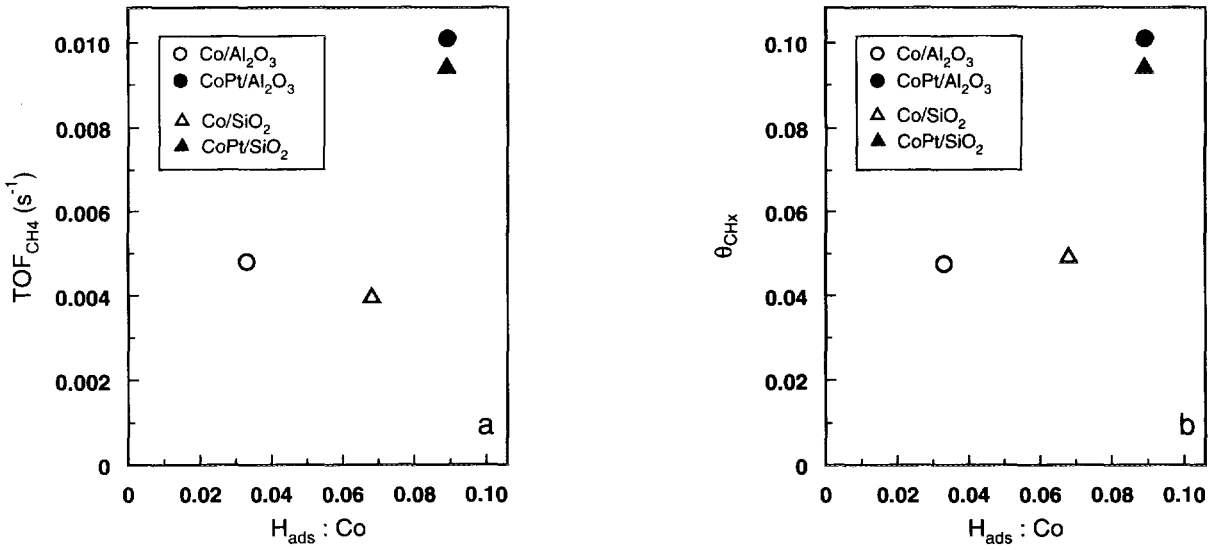

FIG. 5. Kinetic data from steady-state and SSITKA experiments as a function of H_{ads}:Co. T = 483 K, P = 1 bar, H_2/CO = 7.3, 44% inert (Ar) in feed. (a) Apparent turnover frequency for CH_4 formation (TOF_{CH_4}) based on H_{ads}. (b) Surface coverage of reaction intermediates (θ_{CH_x}) leading to CH_4. $\theta_{CH_x} = N_{CH_x}/H_{ads,298K}$.

motion is the main reason for the observed effect on Al_2O_3-supported catalysts. The highly dispersed, but difficult to reduce, surface cobalt oxide phase is almost completely reduced in Co–Pt/Al_2O_3, whereas only the larger Co_3O_4 particles are reduced on Co/Al_2O_3. An increase in the dispersion of metallic cobalt on Co–Pt/Al_2O_3 compared to monometallic Co/Al_2O_3 is observed as a result of averaging the dispersion of two cobalt phases of different dispersions. On SiO_2-supported catalysts, the presence of Pt does not influence the final extent of reduction and gives only a moderate increase in cobalt dispersion.

Steady-state and transient kinetic experiments indicate constant intrinsic turnover frequency for CO hydrogenation on these catalysts, independent of the type of support and the presence of Pt.

ACKNOWLEDGMENTS

The Norwegian Research Council and Statoil are gratefully acknowledged for financial support, and the authors thank Tarald Taraldsen for performing the XRD measurements, and Astrid Lydro for performing chemisorption measurements.

REFERENCES

1. Goodwin, J. G., Jr, *Prepr. Am. Chem. Soc. Div. Petr. Chem.* **36,** 156 (1991).
2. Guczi, L., Hoffer, T., Zsoldos, Z., Zyade, S., Maire, G., and Garin, F., *J. Phys. Chem.* **95,** 802 (1991).
3. Iglesia, E., Soled, S. L., and Fiato, R. A., *J. Catal.* **137,** 212 (1992).
4. Johnson, B. G., Bartholomew, C. H., and Goodman, D. W., *J. Catal.* **128,** 231 (1991).
5. Batley, G. E., Ekstrom, A., and Johnson, D. A., *J. Catal.* **34,** 368 (1974).
6. Belousov, V. M., Stoch, J., Batcherikova, I.V., Rozhkova, E.V., and Lyashenko, L.V., *Appl. Surf. Sci.* **35,** 481 (1988).
7. Sass, A. S., Shvets, V. A., Savel'eva, G. A., and Kazanskii, V. B., *Kinet. Katal.* **26,** 1149 (1985).
8. Zsoldos, Z., Hoffer, T., and Guczi, L., *J. Phys. Chem.* **95,** 795 (1991).
9. Zsoldos, Z., and Guczi, L., *J. Phys. Chem.* **96,** 9393 (1992).
10. Zyade, S., Garin, F., and Maire, G., *New J. Chem.* **11,** 429 (1987).
11. van't Blik, H. F. J., Koningsberger, D. C., and Prins, R., *J. Catal.* **97,** 210 (1986).
12. van't Blik, H. F. J., and Prins, R., *J. Catal.* **97,** 188 (1986).
13. Dees, M. J., and Ponec, V., *J. Catal.* **119,** 376 (1989).
14. Bardi, U., Beard, B. C., and Ross, P. N., *J. Catal.* **124,** 22 (1990).
15. Bardi, U., Atrei, A., Cortigiani, B., Rovida, G., and Torrini, M., *Surf. Sci. Lett.* **282,** L365 (1993).
16. Takeuchi, K., Matsuzaki, T., Arakawa, H., and Sugi, Y., *Appl. Catal.* **18,** 325 (1985).
17. Takeuchi, K., Matsuzaki, T., Arakawa, H., Hanaoka, T., and Sugi, Y., *Appl. Catal.* **48,** 149 (1989).
18. Matsuzaki, T., Takeuchi, K., Arakawa, H., Hanaoka, T., and Sugi, Y., *Catal. Sci. Technol.* **1,** 249 (1991).
19. Takeuchi, K., Matsuzaki, T., Arakawa, H., Hanaoka, T., Sugi, Y., and Wei, K. M., *J. Mol. Catal.* **55,** 361 (1989).
20. Guczi, L., Matusek, K., and Bogyay, I., *C1 Mol. Chem.* **1,** 355 (1986).
21. Lapidus, A. L., Krylova, A. Y., Kozlova, G. V., Kondrat'ev, L. T., Myshenkova, T. N., Babenkova, L. V., Kul'evskaya, Y. G., and Sominskii, S. D., *Izv. Akad. Nauk. SSSR Ser. Khim.* **3,** 521 (1990).
22. Biloen, P., Helle, J. N., van den Berg, F. G. A., and Sachtler, W. M. H., *J. Catal.* **81,** 450 (1983).
23. Mirodatos, C., *Catal. Today* **9,** 83 (1991).
24. Blekkan, E. A., Holmen, A., and Vada, S., *Acta Chem. Scand.* **47,** 275 (1993).
25. Bartholomew, C. H., and Farrauto, R. J., *J. Catal.* **45,** 41 (1976).
26. Jones, R. D., and Bartholomew, C. H., *Appl. Catal.* **39,** 77 (1988).
27. Yang, C.-H., Soong, Y., and Biloen, P., *in* "Proceedings 8th International Congress on Catalysis, Berlin, 1984" Vol. 2, p. 3. Dechema, Frankfurt-am-Main, 1984.
28. Hoost, T. E., and Goodwin, J. G., Jr., *J. Catal.* **137,** 22 (1992).

29. de Pontes, M., Yokomizo, G. H., and Bell, A. T., *J. Catal.* **104,** 147 (1987).
30. Arnoldy, P., and Moulijn, J. A., *J. Catal.* **93,** 38 (1985).
31. Tung, H.-C., Yeh, C.-T., and Hong, C.-T., *J. Catal.* **122,** 211 (1990).
32. Wang, W.-J., and Chen, Y.-W., *Appl. Catal.* **77,** 223 (1991).
33. Hoff, A., Blekkan, E. A., Holmen, A., and Schanke, D., *in* "Proceedings 10th International Congress on Catalysis, Budapest, 1992" (L. Guczi, F. Solymosi, and P. Tetenyi, Eds.), p. 2067. Akadémiai Kiadó, Budapest, 1993.
34. Hoff, A., Ph.D. Thesis, University of Trondheim, 1993.
35. Okamoto, Y., Adachi, T., Nagata, K., Odawara, M., and Imanaka, T., *Appl. Catal.* **73,** 249 (1991).
36. van't Blik, H. F. J., and Prins, R., *J. Catal.* **97,** 188 (1985).
37. Bruce, L., Hoang, M., Hughes, A. E., and Turney, T. W., *Appl. Catal. A General* **100,** 51 (1993).
38. Iglesia, E., Soled, S. L., Fiato, R. A., and Via, G. H., *J. Catal.* **143,** 345 (1993).
39. Bartholomew, C. H., and Reuel, R. C., *Ind. Eng. Chem. Prod. Res. Dev.* **24,** 56 (1985).
40. Bartholomew, C. H., and Pannell, R. B., *J. Catal.* **65,** 390 (1980).
41. Reuel, R. C., and Bartholomew, C. H., *J. Catal.* **85,** 63 (1984).
42. Castner, D. G., Watson, P. R., and Chan, I. Y., *J. Phys. Chem.* **94,** 819 (1990).
43. Lee, J.-H., Lee, D.-K., and Ihm, S.-K., *J. Catal.* **113,** 544 (1988).
44. Lee, W. H., and Bartholomew, C. H., *J. Catal.* **120,** 256 (1989).